Predictive Current Control with Reactive Power Minimization in Six-phase Wind Energy Generator using Multi-Modular Direct Matrix Converter

Sergio Toledo and Marco Rivera
Department of Electrical Engineering
Universidad de Talca
Curicó, Chile

Raúl Gregor, Jorge Rodas and Leonardo Comparatore
Laboratory of Power and Control Systems
Universidad Nacional de Asunción
Luque, Paraguay

Abstract—Increasing worldwide energy demand and well known pollution effects of fossil fuels, make necessary to develop new environmentally friendly energy generation systems such as wind energy. In this research a predictive current control with reactive power reduction is proposed for a six-phase energy generator - multi-modular matrix converter system. The proposal shows a significant harmonic reduction in the generator side and a THD less than 0.6% at the load side, with good current tracking, making it suitable for further grid interconnection.

Index Terms—Multi-modular matrix converter, multiphase generator, predictive control, wind generation.

I. Introduction

Owning to the well-known detrimental effect over the environment of fossil fuels, nowadays worldwide energy generation focus has shifted to generating power from renewable energy sources (RES) [1]. In the field of RES, a very active research area is focused in the multiphase wind energy generator (MWEG) systems [2]. In particu lar, MWEG with multiple three-phase windings are very convenient for wind turbine (WT) and several studies employing these topologies have been conducted recently [3]. The main reasons of multiphase choice for WT are the possibility to split the power and the current between a higher numbers of phases, allowing the per-phase inverter power rating reduction, consequently, power semiconductors with lower power rates can be used [4]. Furthermore, this configuration guarantees WT working continuity, even in presence of phase and/or inverter faults [5]. Hence, the use of multiphase electrical drives in WT should enable to increase the availability, the working time, and consequently, the annual energy yield. In MWEG, the six-phase wind energy generator (SpWEG) is probably one of the most widely discussed topology [3]. Over all the possibilities in power converters present in the literature, fully rated back-to-back converter is the most used in actual applications [6]. However, these converters required storage energy elements (i.e. capacitor banks) which provide weight, volume and failure possibilities to the power converter stage. Recent research efforts have been focused in the development of a flexible power interfaces based on a modular architecture capable to interconnecting different RES [2].

These efforts converge in the multi-modular matrix converter (MMMC) topologies whose main feature is the ability to provide a three-phase sinusoidal voltages with variable amplitude and frequency using fully controlled bi-directional switches without the use of storage energy elements [7].

Ideally a matrix converter (MC) should feed the load with sinusoidal currents while generating sinusoidal input currents with controlled power factor to the mains [8]. Model-based predictive control (MPC) was introduced in the late seventies and in recent years it has been introduced for power converters and has been used for different applications [9], showing in several cases better performance than the classic PWM modulation techniques [10].

Considering the above background, the main contribution of this paper comparing to previous works is focused on a theoretical performance analysis of a MMMC combined with a SpWEG intended for ensure an efficient current control with source reactive power minimization, in order to reduce the harmonic injection both the load and towards the generator.

In Section II SpWEG model is briefly described. Then, Section III shows the model of the conversion system. The main contribution is shown in Section IV, presenting the proposed cost function and control design. Afterwards, in Section V, simulation results are depicted and finally, concluding remarks are summarized in Section VI.

II. Six-phase wind energy generator model

The mathematical model of the SpWEG is very similar to the six-phase induction motor model, with differences in the SpWEG has a capacitor bank connected to its stator terminals, which must be considered in the model of the generator, and in this case, rotor speed, provided by the turbine is considered as input, and not output as the motor case. A detailed explanation of the generator model is not included here for sake of conciseness and can be found in [11]. As the stator of the self-excited SpWEG is connected to an isolated load, the magnetizing inductance and stator magnetizing current cannot be considered constant. The variation of the magnetizing inductance is the main factor for the generation of voltage build-up and stabilization. It consists in a nonlinear function,
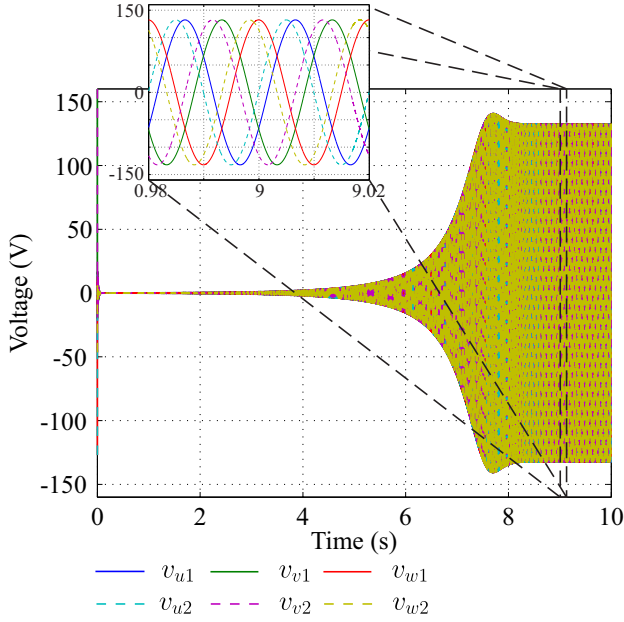
Fig. 1. Build-up voltage of the self-excited SpWEG.

which can be represented by a second order polynominal curve fit as:

$$L_m = -0.0213\,I_m^2 + 0.0631\,I_m + 0.1774,$$
$$0 < I_m < 2.9\,\text{A}, \qquad (1)$$

being $I_m = \sqrt{(i_{\alpha s} + i_{\alpha r})^2 + (i_{\beta s} i_{\beta r})}$.

Using the mentioned mathematical model and the approximated L_m function described in (1), voltage build-up and stationary state six-phase voltages for a mechanical rotor speed ω_m of 1,000 rpm are depicted in Fig. 1. Under these conditions it is possible to observe that the stationary state is reached in about 8 s. Phase voltage of the SpWEG is 130 V with a frequency f of 50 Hz. The generator supplied voltages connected to N_1 (Fig. 2), are represented by v_{u1}, v_{v1} and v_{w1}. Analogously, v_{u2}, v_{v2} and v_{w2} represent generator supplied voltages of the phases connected to N_2.

III. MODEL OF THE POWER CONVERSION SYSTEM

The topology for power control is presented in Fig. 2. It consists in two three-phase MC modules connected to the SpWEG by a (RLC) input filter and then connected to the load by an output filter. In order to simplify the analysis, follow vectorial representations are used:

$$\mathbf{v}_s = \begin{bmatrix} v_{uj} \\ v_{vj} \\ v_{wj} \end{bmatrix}, \quad \mathbf{i}_s = \begin{bmatrix} i_{uj} \\ i_{vj} \\ i_{wj} \end{bmatrix} \quad j \in \{1,2\}, \qquad (2)$$

where j indicates the respective module. Vector $\mathbf{v}_i$ refers to input filter voltages and $\mathbf{i}_i$ to currents. On the other hand, $\mathbf{v}_o$ represents MC output voltages applied to output filter and $\mathbf{i}_o$ to currents. Finally, $\mathbf{v}_g$ represents load voltages, and $\mathbf{i}_g$ is the vector of load currents. In the case of $\mathbf{v}_g$ j index

refers to whether the voltage is measured from N_1 or N_2. The MC power topology is composed of nine bi-directional power switches, which can generate 27 feasible switching states [12]. Following equations relate the input and output voltages or currents in terms of the switching states of the MC [12]:

$$\mathbf{v}_o = \mathbf{S}\mathbf{v}_i, \quad \mathbf{i}_i = \mathbf{S}^T\mathbf{i}_o, \quad \mathbf{S} = \begin{bmatrix} S_{ua} & S_{ub} & S_{uc} \\ S_{va} & S_{vb} & S_{vc} \\ S_{wa} & S_{wb} & S_{wc} \end{bmatrix} \qquad (3)$$

being $\mathbf{S}$ the instantaneous transfer matrix, where the S_{xy} element has a binary value, corresponding to the state of the single switch. The model of the passive output filter is defined as:

$$\mathbf{v}_o - \mathbf{v}_g = L_o \frac{d\mathbf{i}_o}{dt} + R_o\mathbf{i}_o, \qquad (4)$$

where L_o and R_o represent the output inductance and resistance, respectively. In the case of the input filter, the dynamic behavior can be directly modeled by using the space-state representation approach as:

$$\frac{d}{dt}\begin{bmatrix} \mathbf{v}_i \\ \mathbf{i}_s \end{bmatrix} = \mathbf{A}_c \begin{bmatrix} \mathbf{v}_i \\ \mathbf{i}_s \end{bmatrix} + \mathbf{B}_c \begin{bmatrix} \mathbf{v}_s \\ \mathbf{i}_i \end{bmatrix}, \qquad (5)$$

where:

$$\mathbf{A}_c = \begin{bmatrix} -\frac{1}{R_pC_f} & \frac{1}{C_f} \\ -\frac{1}{L_f} & -\frac{R_f}{L_f} \end{bmatrix}, \quad \mathbf{B}_c = \begin{bmatrix} \frac{1}{R_pC_f} & -\frac{1}{C_f} \\ \frac{1}{L_f} & 0 \end{bmatrix}, \qquad (6)$$

being L_f, C_f and R_p the filter inductance, capacitance and resistance. R_f represents the leakage resistance of L_f.

IV. PROPOSED CONTROL STRATEGY

In this paper, The discrete model of the system is derived from the continuous time linear system represented by (4) and (5).

The output filter current prediction for each module is calculated using the forward Euler discretization of (4), as follows:

$$\mathbf{i}_o(k+1) = \left(1 - \frac{R_oT_s}{L_o}\right)\mathbf{i}_o(k) + \frac{T_s}{L_o}\left(\mathbf{v}_o(k) - \mathbf{v}_g(k)\right), \quad (7)$$

where T_s is the sampling time, $\mathbf{i}_o(k)$ and $\mathbf{v}_g(k)$ are measured, and $\mathbf{v}_o(k)$ is calculated for all switch combinations to predict the next value of the output currents and evaluate the cost function in order to select the combination that minimizes this function. On the other hand, the discrete model for the input filter is given by:

$$\begin{bmatrix} \mathbf{v}_i(k+1) \\ \mathbf{i}_s(k+1) \end{bmatrix} = \mathbf{\Gamma} \begin{bmatrix} \mathbf{v}_i(k) \\ \mathbf{i}_s(k) \end{bmatrix} + \mathbf{\Phi} \begin{bmatrix} \mathbf{v}_s(k) \\ \mathbf{i}_i(k) \end{bmatrix} \qquad (8)$$

with $\mathbf{\Gamma} = e^{\mathbf{A}_cT_S}$ and $\mathbf{\Phi} = \int_0^{T_s} e^{\mathbf{A}_C(T_s-\tau)}\mathbf{B}_cd\tau$.

In this case, the control criteria is the regulation of load current with minimum reactive power on the generator side. To achieve this, the reference currents for each modules are defined as half of the desired total current, that is $\mathbf{i}_o^* = 0.5\,\mathbf{i}_g^*$, where $\mathbf{i}_o^*$ represents the desired current supplied for each module, while $\mathbf{i}_g^*$ is the reference current.

Thereafter, the predicted errors are computed for each possible switching vectors and then, the cost function is evaluated.
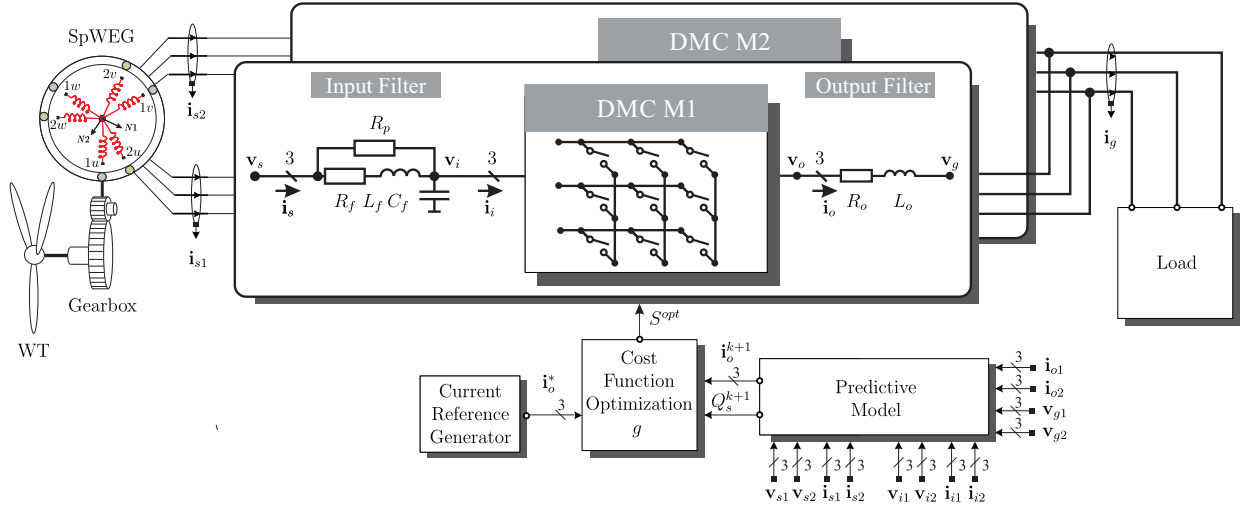
Fig. 2. Current predictive control with reactive power minimization in SpWEG using multi-modular direct matrix onverter topology.

TABLE I
SYSTEM AND CONTROLLER PARAMETERS.

Parameter	Simulation parameters		
	Symbol	Value	Unit
Load resistance	R	10	Ω
Load inductance	L	30	mH
Input filter leakage resistance	R_f	10	mΩ
Input filter inductance	L_f	30	mH
Input filter capacitance	C_f	6.9	μF
Output filter resistance	R_o	10	mΩ
Output filter inductance	L_o	30	mH
Sampling time	T_s	10	μs

This cost function (g) provides to the predictive control algorithm the ability of incorporating different objectives. In order to reduced the number of calculations, the whole variables are transformed to his $\alpha - \beta$ components applying Clarke's transformation [13]. Subscript p represents the predicted value of the variables for each feasible switching combination while the other variables are measured in the instant k. From the evaluation of all the possible switching vectors, the algorithm selects the one which minimizes g and applies it in the next sample time. Thus, proposed cost function is given by:

$$
\begin{aligned}
g &= g_1 + g_2 + \lambda_1 g_3 + \lambda_2 g_4, \\
g_1 &= \left(i_{\alpha 1}^* - i_{\alpha 1p}\right)^2 + \left(i_{\beta 1}^* - i_{\beta 1p}\right)^2, \\
g_2 &= \left(i_{\alpha 2}^* - i_{\alpha 2p}\right)^2 + \left(i_{\beta 2}^* - i_{\beta 2p}\right)^2, \qquad (9) \\
g_3 &= \left(v_{s\alpha 1}\, v_{s\beta 1p} - v_{s\beta 1}\, i_{s\alpha 1p}\right)^2, \\
g_4 &= \left(v_{s\alpha 2}\, i_{s\beta 2p} - v_{s\beta 2}\, i_{s\alpha 2p}\right)^2,
\end{aligned}
$$

where $i_{\alpha 1,2}$, $i_{\alpha 1,2}$ are obtained from $\mathbf{i}_o$ in modules 1 and 2. The same for predicted current that have subscript p and the generator voltages and currents. The weights for reactive power minimization in the cost function are λ_1 and λ_2.

V. SIMULATION RESULTS

The proposed control strategy was simulated using Matlab/Simulink environment. Table I shows simulation parameters. In Fig. 3 current tracking is presented. At the beginning, desired current has set to 5 A. At 9 s, desired current changes to 3 A and a good tracking is observed. In a second simulation, λ_1 and λ_2 have been set to zero until 9 s with desired current set to 5 A. Then λ_1 and λ_2 are set to 0.00008. This means no reactive power control is applied before that time. Fig 4 and Fig 5 show the performance of modules 1 and 2, respectively. As may be seen, i_g tracks successfully to i_g^* (in both figures it is depicted for phase a). In the enlarged square it can be appreciated the effects of the switching, resulting in some harmonic in the load. Furthermore, it is presented generator voltages versus currents for phase u in order to appreciate the effect of the reactive power minimization. It can be seen that the power quality presents a noticeable improvement. Furthermore, for every module, reactive power are presented to appreciate the reduction reach with the proposal. Maximum phase total harmonic distortion (THD) over the load is 0.53 % before reactive minimization, then it reduces to 0.48 %. In the generator side, THD shows a reduction from 50.2 % to 6.4 % after reactive power minimization.

VI. CONCLUSION

The proposed predictive control scheme shows a good performance in terms of current control and harmonics mitigation, both in the generator side as well as in load side. The proposed control strategy can be extrapolated for more modules, always being careful in not to exceed the processing capacity of the control element. The simulation results are promising and is expected to reach the experimental implementation in a short time and extend the concept in grid interconnection. THD has been less than 0.48 % in the load and has shown a reduction from 50.2% to 6.4% in the generator side. A good power quality is shown both in load side as well as generator side
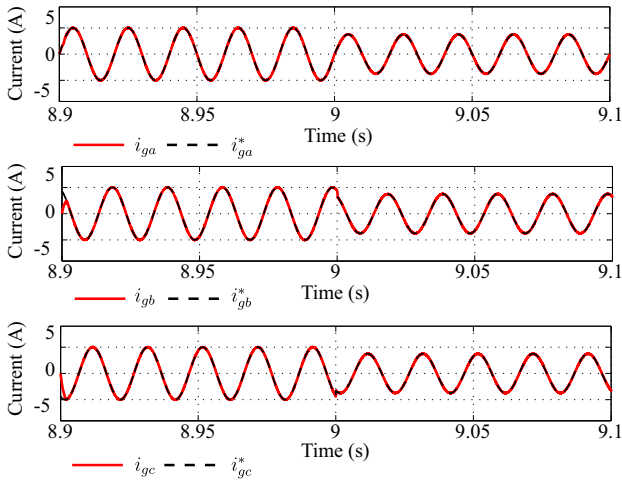
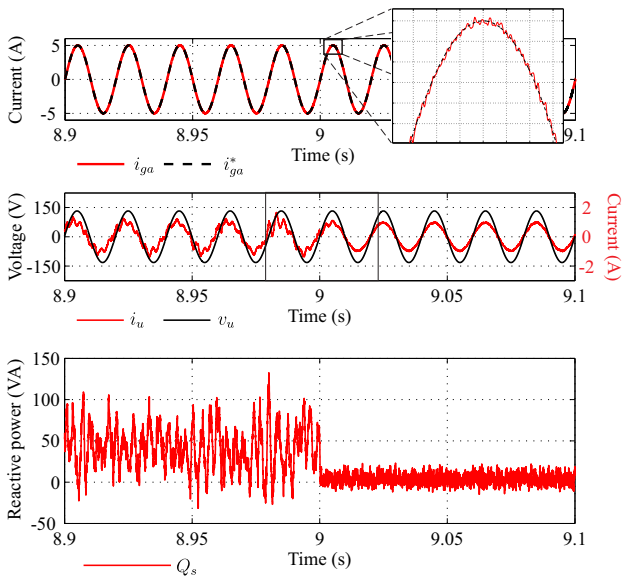Fig. 3. Current tracking in the load from 5 (A) to 3 (A) reference change.

Fig. 4. Module 1 performance. From top to bottom: current tracking, generator voltage and current and finally, reactive power in the source.

Fig. 5. Module 2 performance. From top to bottom: current tracking, generator voltage and current and finally, reactive power in the source.

with a correct desired load current tracking. This is promising and makes the topology suitable for future grid connection.

REFERENCES

[1] International Energy Agency (IEA), "Renewable energy medium-term market report 2015. Market Analysis and Forecasts to 2020 - Executive Summary," Paris, Tech. Rep., 2015.

[2] M. J. Duran and F. Barrero, "Recent Advances in the Design, Modeling, and Control of Multiphase Machines - Part II," *IEEE Transactions on Industrial Electronics*, vol. 63, no. 1, pp. 459–468, 2016.
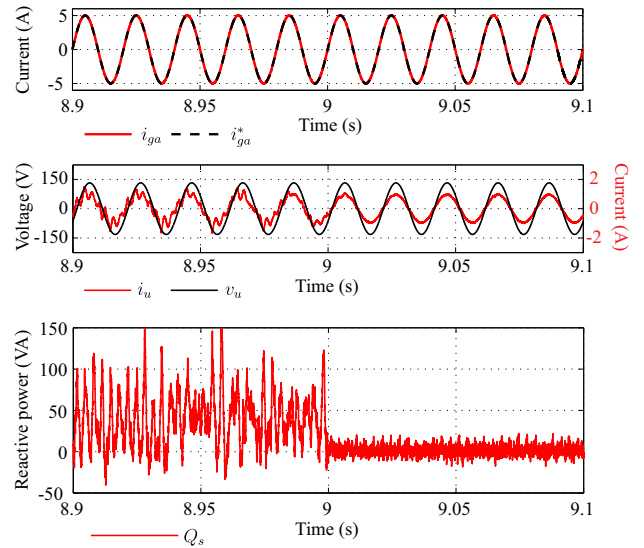
[3] B. V. Yaramasu, B. Wu, P. C. Sen, S. Kouro, and M. Narimani, "High-Power Wind Energy Conversion Systems : State-of-the-Art and Emerging Technologies," *Proceedings of the IEEE*, vol. 103, no. 5, pp. 740–788, 2015.

[4] I. Lopez, S. Ceballos, J. Pou, J. Zaragoza, J. Andreu, I. Kortabarria, and V. G. Agelidis, "Modulation Strategy for Multiphase Neutral-Point-Clamped Converters," *IEEE Transactions on Power Electronics*, vol. 31, no. 2, pp. 928–941, 2016.

[5] M. J. Duran, I. Gonzalez Prieto, M. Bermudez, F. Barrero, H. Guzman, and M. R. Arahal, "Optimal Fault-Tolerant Control of Six-Phase Induction Motor Drives with Parallel Converters," *IEEE Transactions on Industrial Electronics*, vol. 63, no. 1, pp. 629–640, 2016.

[6] I. Gonzalez-Prieto, M. J. Duran, H. S. Che, E. Levi, M. Bermúdez, and F. Barrero, "Fault-tolerant Operation of Six-phase Energy Conversion Systems with Parallel Machine-Side Converters," *IEEE Transactions on Power Electronics*, vol. 31, no. 4, pp. 3068–3079, 2016.

[7] Y. Sun, W. Xiong, M. Su, X. Li, H. Dan, and J. Yang, "Carrier-Based Modulation Strategies for Multimodular Matrix Converters," *IEEE Transactions on Industrial Electronics*, vol. 63, no. 3, pp. 1350–1361, 2016.

[8] M. Vijayagopal, P. Zanchetta, L. Empringham, L. D. Lillo, and P. Wheeler, "Modulated Model Predictive Current Control for Direct Matrix Converter with Fixed Switching Frequency," in *Power Electronics and Applications (EPE'15 ECCE-Europe), 2015 17th European Conference on*, 2015, pp. 1–10.

[9] M. Rivera, P. Wheeler, and A. Olloqui, "Predictive Control in Matrix Converters - Part II : Control Strategies , Weaknesses and Trends," in *2016 IEEE International Conference on Industrial Technology (ICIT)*, 2016, pp. 1098–1104.

[10] J. Holtz, "Advanced PWM and Predictive Control — An Overview," *IEEE Transactions on Industrial Electronics*, vol. 63, no. 6, pp. 3837–3844, 2016.

[11] J. Rodas, R. Gregor, Y. Takase, D. Gregor, and D. Franco, "Multi-Modular Matrix Converter Topology Applied to the Six-Phase Wind Energy Generator," in *Power Engineering Conference (UPEC), 2015 50th International Universities*, no. 1, 2015, pp. 1–6.

[12] O. Gulbudak, S. Member, E. Santi, and S. Member, "FPGA-Based Model Predictive Controller for Direct Matrix Converter," *IEEE Transactions on Industrial Electronics*, vol. 63, no. 7, pp. 4560–4570, 2016.

[13] L. Zhan, Y. Liu, and Y. Liu, "A Clarke Transformation-based DFT Synchrophasor Algorithm for Wide Frequency Range," *IEEE Transactions on Smart Grid*, vol. PP, no. 99, pp. 1–1, 2016.